Electronic Supplementary Material (ESI) for Journal of Materials Chemistry C.

SUPPLEMENTARY INFORMATION

Localized optical-quality doping of graphene on silicon waveguides through a TFSA-containing polymer matrix

---

Lara Misseeuw[a], Tymoteusz Ciuk[b], Aleksandra Krajewska[b,c], Iwona Pasternak[b,d], Wlodek Strupinski[b,d], Benjamin Feigel[a], Mulham Khoder[a], Isabelle Vandriessche[e], Jürgen Van Erps[a], Sandra Van Vlierberghe[a,f], Hugo Thienpont[a], Peter Dubruel[f], Nathalie Vermeulen[a]*

a. Brussels photonics team (B-PHOT), Dept. of Applied Physics and Photonics (IR-TONA), Vrije Universiteit Brussel, Pleinlaan 2, B-1050 Brussels, Belgium

*lmisseeu@b-phot.org

b. Institute of electronic materials technology, Wolczynska 133, 01-919 Warsaw, Poland

c. Institute of optoelectronics, Military University of Technology, Gen. S. Kaliskiego 2, 00-908 Warsaw, Poland

d. Faculty of Physics, Warsaw University of Technology, Koszykowa 75, 00-662 Warsaw, Poland

e. Sol-gel centre for research on inorganic powders and thin films synthesis, Ghent University, Krijgslaan 281 (S3), B-9000 Ghent, Belgium

f. Polymer Chemistry & Biomaterials research group, Ghent University, Krijgslaan 281 (S4 Bis), B-9000 Ghent, Belgium

Experimental methods

Graphene growth and graphene transfer

Monolayer graphene was provided by chemical vapor deposition (CVD) growth, with methane as carbon precursor, on high-purity polycrystalline copper foil. After covering graphene with a 200 nm-thin layer of PMMA, graphene was transferred via electrochemical delamination onto the substrates [1,2].

In a first stage, graphene was transferred on polished Si samples (1 cm x 1 cm, highly resistive with R > 1000 Ω cm), after which the PMMA was removed.

In a second stage, graphene was transferred onto a silicon on insulator (SOI) photonic chip. The SOI waveguides used are strip waveguides with a height of 220 nm. In-plane light coupling is established using lensed fibers positioned horizontally next to the chip edges. Before PMMA removal, an additional oxygen plasma etching step was necessary using a mechanical mask (with a minimal opening size around 100 µm and an alignment accuracy of 10 µm) to create graphene sections on the waveguides with a length varying between 100 and 300 µm, to obtain graphene-free zones at the tapers [3]. The latter plasma etching step offers additional freedom to adjust the graphene-covered zones on the photonic chip to the desired dimension, size and shape.

Preparation of the TFSA/POFPMA dopant solution

Bis(trifluoromethanesulfonyl)amide (TFSA, $[CF_3SO_2]_2NH$) was selected as the active p-type dopant (Sigma Aldrich, ≥ 95%) and incorporated into a polymer matrix of poly (2,2,3,3,4,4,5,5-octafluoropentyl methacrylate) (POFPMA).

POFPMA was synthesized by a radical UV-induced bulk polymerization reaction as described below. Irgacure 651 (4 mol% relative to the amount of double bonds, BASF) was solubilized as photo-initiator in 2,2,3,3,4,4,5,5-octafluoropentyl methacrylate (OFPMA, Sigma Aldrich, 98%) and injected in a pre-shaped mould consisting of two teflon foil covered glass plates separated by a silicon spacer (thickness: 1 mm). After two hours UV-irradiation (365 nm, 15 mW/cm^2), the obtained POFPMA polymer was used without further purification steps. Polymer characterization was carried out by differential scanning calorimetry (DSC, Q2000-TA

Instruments with TA universal analysis software), thermogravimetric analysis (TGA, Hi-Res TGA 2950 Thermogravimetric Analyzer (TA Instruments), with TA universal analysis software) and gel permeation chromatography (GPC, with a mixed E, 3 µm (Polymer Laboratories) column (500 – 30000 g/mol) using chloroform ($CHCl_3$) as solvent and PMMA standards and Empower pro software. The detection was performed using a 2414 RI system (Waters).

TFSA (the active p-type dopant, with a concentration varying between 0 and 40 mM) and POFPMA (the polymer matrix) were solubilized in a suitable solvent. In the case of TFSA/POFPMA doping on graphene on top of Si samples by spin coating, a concentration of 20 w/v% POFPMA was dissolved in acetone. When applying TFSA/POFPMA doping on top of graphene on the SOI photonic chip by inkjet printing, 20 w/v% POFPMA was dissolved in OFPMA as solvent.

Deposition of the TFSA/POFPMA dopant

Spin coating was applied to deposit TFSA/POFPMA on flat graphene/Si samples. The applied spin coating parameters included a spin speed of 5000 rpm, an acceleration of 1000 rpm/s, a spin time of 30 s and an applied volume of 20 µl.

To enable localized doping of each waveguide on the SOI chip separately, we applied inkjet printing of the dopant solution. The localized doping of graphene was performed using a drop-on-demand inkjet printer with piezo-electric inkjet technology (Dimatix Materials Printer DMP-2831, FUJIFILM), with a drive voltage of 21 V and a drop spacing of 20 µm. 3D structures were produced by accurately positioning the ejected droplets in a layer-by-layer fashion.

Characterization of the deposited TFSA/POFPMA dopant layer

Firstly, we investigated the quality of the spin coated TFSA/POFPMA layers. The surface morphology (expressed in RMS roughness) was characterized with atomic force microscopy (AFM), using a multimode scanning probe microscope (Digital Instruments) equipped with a Nanoscope IIIa controller. The scanned surface was recorded in tapping mode with a scan rate of 0.2 Hz and a silicon cantilever (OTESPA-Veeco). Nanoscope software version 4.43r8 was used for surface roughness analysis after the recorded images were modified with an X and Y Plane Fit Auto procedure. The chemical composition and homogeneity of the obtained layers

was determined using X-ray photo-electron spectroscopy (XPS) measurements on three random locations on undoped graphene on a Si sample (reference) and on a TFSA/POFPMA doped graphene (ESCA S-probe VG monochromatic spectrometer with an Al Kα X-ray source (1486 eV), recorded with a spot size of 250 µm by 1000 µm and analyzed using Casa XPS software package). The transparency of the layers was quantified by optical transmission measurements of the dopant layer spin coated on glass slides (Jasco V-670 UV-VIS/NIR Spectrophotometer over the wavelength range from 550 to 1900 nm, including both the VIS (visible spectrum) and NIR (near infrared) with Spectra Manager™ software). The layer thickness of the spin coated TFSA/POFPMA layer was determined with ellipsometry (J.A. Woollam Co., M-2000 with CompleteEASE® software).

Secondly, we analyzed the inkjet printed TFSA/POFPMA lines via AFM for determination of the layer roughness and via stylus profilometry (Dektak (Bruker) with Bruker's Vision64 software) for the printed lines height determination. We also carried out linear optical transmission measurements of the dopant printed on a waveguide of the SOI chip without graphene, to check dopant-induced propagation losses as compared with the linear optical transmission of Si waveguides without doping. A continuous wave Yenista laser at the telecom wavelength of 1550 nm was used to execute the transmission measurements, with an input power of 1 mW.

Graphene doping quantification

As graphene was applied on two different types of substrates (flat Si and SOI waveguides), we employed two methods for determining the doping efficiency.

Via a Hall effect measurement system in van der Pauw geometry (0.55T Ecopia HMS-3000 Hall setup), we could measure the electrical parameters of graphene transferred on flat Si samples (i.e. charge carrier concentration (n in cm^{-2}), the mobility (µ in $cm^2\ V^{-1}\ s^{-1}$) and the sheet resistance (Rs in Ω/sq)). After placing four indium contacts in the corners of the graphene-covered Si samples, we performed Hall measurements on the graphene before and after spin coating the TFSA/POFPMA doping layer.

For TFSA/POFPMA applied on a Si waveguide of the SOI photonic chip, the doping efficiency was determined by the change in optical transmission for the quasi-Transverse Electric waveguide mode when comparing a graphene-covered Si waveguide with and without

TFSA/POFPMA dopant. These tests were performed by a continuous wave Yenista laser at a telecom wavelength of 1550 nm, with an input power of 1 mW.

To extract the graphene doping level from the waveguide transmission tests, we calculated the change in graphene's Fermi level required to obtain the observed increase in transmission after doping. Hereto, we used the commercial mode solver Lumerical MODE which allows calculating the transmission loss of the waveguide's modes as a function of graphene's Fermi level. In the Lumerical MODE software, the graphene was modeled as a two-dimensional material with an electronic scattering rate of 33 meV, and we assumed that only the waveguide's top surface was covered with graphene. The TFSA doping layer covering the graphene was modeled as a dielectric with a refractive index of 1.49 (cfr. PMMA).

p-doping effect of protonic acids as a function of their acidity

Acids are commonly used dopants; the acidic protons are strong electron acceptors which can realize a charge transfer, resulting in lowering graphene's chemical potential. Since POFPMA serves as polymer matrix to ensure the optical quality and stability of the dopants, we studied the doping efficiency of several acids with different acidity strength (expressed in pK_a), incorporated in the POFPMA layer [4]: H_3PO_4 (pK_a = 2.1), HNO_3 (pK_a = -1.7), H_2SO_4 (pK_a = -2.5), HBr (pK_a = -4.9), HI (pK_a = -7.7) and TFSA (pK_a = -11.9), each acid with a concentration of 20 mM and applied to three samples via spin coating onto graphene, transferred on Si samples. By monitoring graphene's electrical parameters with Hall measurements before and after doping, we noticed that monovalent acids (HNO_3, HBr, HI, TFSA) exhibit a stronger p-doping effect according to their acidity strength. H_2SO_4 and H_3PO_4 offer higher doping efficiency as expected, based on their pK_a values, due to their divalent and trivalent acidic nature, respectively. TFSA, considered as a super acid with a pKa of -11.9, is the most promising candidate to optimize the p-doping of graphene.

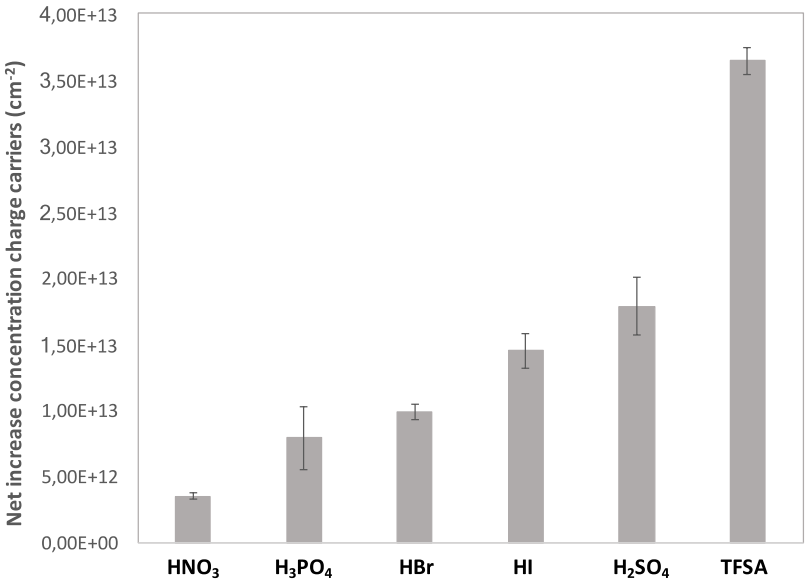

Figure S1. Doping efficiency of several protonic acids (20 mM) with different acidity strengths, mixed with the POFPMA polymer (20 w/v%) in acetone, and spin coated on graphene. Each dopant solution is applied to three different samples.

Scanning electron microscopy (SEM) images of the TFSA/POFPMA dopant layer spin coated on a flat graphene-covered Si sample

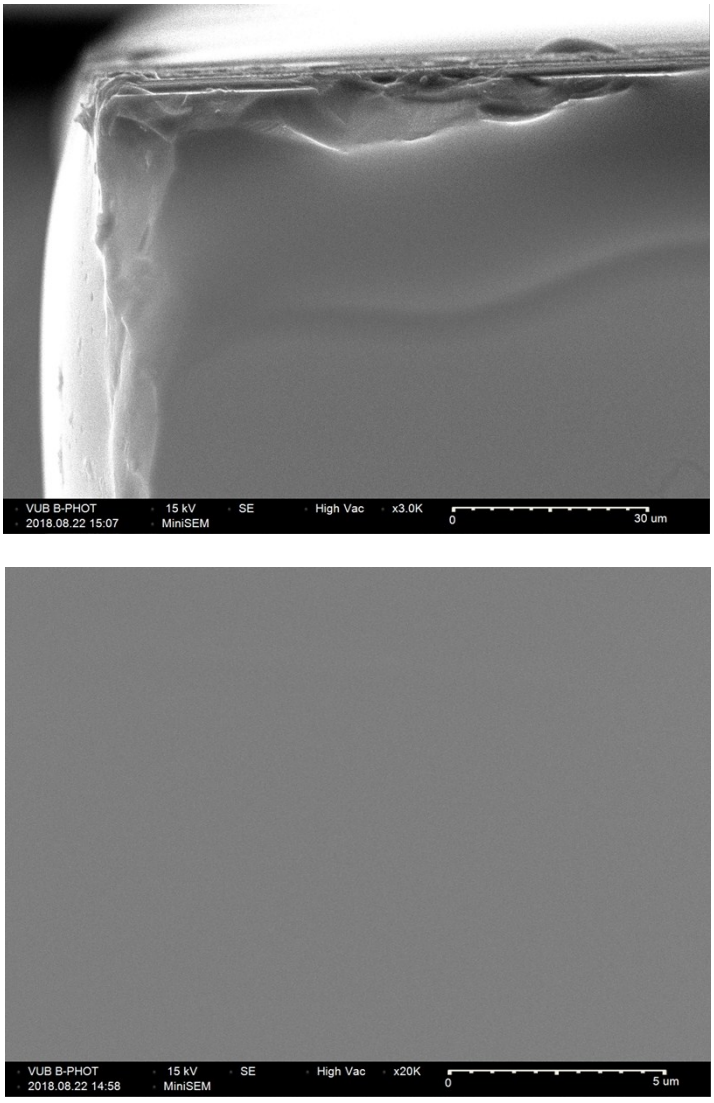

Figure S2. SEM (SNE-4500M (Hirox), with a 12 nm thick gold layer deposited prior to measurement) image of the TFSA/POFPMA dopant layer spin coated on a flat graphene-covered Si sample.

SEM images of the TFSA/POFPMA layer spin coated on graphene clearly revealed the uniform, smooth and cluster-free surface of the dopant layer. The images confirmed the uniformity as observed by optical microscopy and the low surface roughness demonstrated by AFM measurements. The picture above (taken at the upper left corner of the Si sample (1 cm x 1 cm)) was added to indicate that we are properly focusing on the surface.

Table S1. The electrical parameters n, μ and Rs for nine different samples of graphene (CVD grown on copper and transferred to Si substrates) before and after doping with TFSA/POFPMA layer when varying the concentration of TFSA from 0-40 mM.

	Concentration Charge Carriers			Mobility			Sheet Resistance			
Concentration TFSA	n_{before}	n_{after}	Δn	μ_{before}	μ_{after}	Δμ	Rs_{before}	Rs_{after}	ΔRs	Decrease Rs
(mM)	(cm^{-2})	(cm^{-2})	(cm^{-2})	($cm^2 V^{-1} s^{-1}$)	($cm^2 V^{-1} s^{-1}$)	($cm^2 V^{-1} s^{-1}$)	(Ω/sq)	(Ω/sq)	(Ω/sq)	(%)
40	2.89E+12	4.01E+13	3.72E+13	1235	386	-849	1751	403	-1348	77.0
20	2.23E+12	3.84E+13	3.62E+13	1461	950	-511	1917	500	-1417	73.9
15	3.10E+12	4.15E+13	3.84E+13	1229	413	-816	1641	364	-1277	77.8
10	2.86E+12	4.12E+13	3.84E+13	1249	436	-813	1749	347	-1402	80.2
5	5.06E+12	3.01E+13	2.50E+13	773	362	-411	1595	574	-1021	64.0
2.5	4.40E+12	2.14E+13	1.70E+13	993	534	-459	1427	547	-880	61.7
1	5.57E+12	1.61E+13	1.05E+13	828	696	-132	1353	558	-795	58.8
0.5	5.65E+12	1.12E+13	5.57E+12	1434	1249	-185	770	446	-324	42.1
0	2.23E+12	3.64E+12	1.41E+12	1461	1376	-85	1717	1246	-471	27.4

Layer thickness of spin coated POFPMA layer in function of spin speed

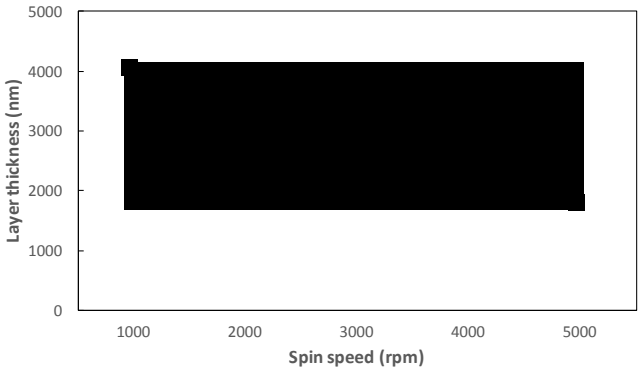

Figure S3. Layer thickness of POFPMA layers spin coated on graphene in function of spin speed (rpm), measured by ellipsometry.

Stability of TFSA/POFPMA doping effect spin coated on graphene

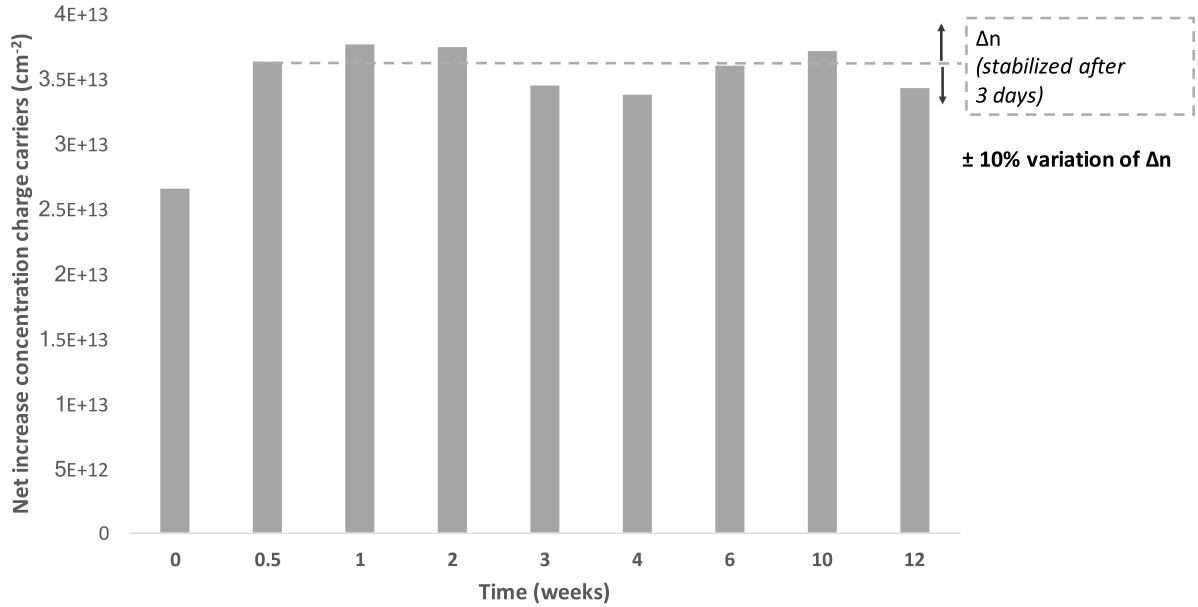

Figure S4. Change in charge carrier concentration (Δn in cm^{-2}), starting from CVD grown graphene on copper followed by transfer to Si substrates and subsequent doped with a TFSA/POFPMA layer (40 mM), monitored as a function of time to verify its doping stability: After three days, the doping is stabilized at its maximum increase in concentration of charge carriers. During the following weeks, the concentration of charge carriers is changing with less than 10% of its maximal Δn value.

Doping capacity of printed TFSA/POFPMA deposition on graphene-covered flat Si substrate

We have performed doping experiments onto flat graphene-covered Si substrates by inkjet-printing TFSA/POFPMA (40 mM TFSA with 20 w/V% in liquid OFPMA). The graphene surface was 1 cm x 1 cm and we have printed 20 lines (each line consisted of three layers), with every line having a surface coverage of 1 cm x 150 µm (L x W). An optical microscopy image of a zoomed-in region is presented in Figure S5. The total coverage of the printed dopant deposition was around 30% of the graphene surface. Measuring the electrical parameters with Hall measurements, prior and after inkjet-printed doping, revealed that the printed deposition resulted in p-doping with an increase in charge carrier concentration and a decrease in sheet resistance, as we expected and which is in agreement with the trend observed for the spin

coated doping strategy. Subsequently, we observed that the change in charge carrier concentration for the samples with the printed lines was proportional to the change in charge carrier concentration for the samples with the spin coated layer multiplied by the surface coverage of the printed lines (see Table S2). E.g. $\Delta n = 1.42 \times 10^{13}$ cm^{-2} (see Table S2) is indeed quite close to 30% of the $\Delta n = 3.72 \times 10^{13}$ cm^{-2} (see Table S1).

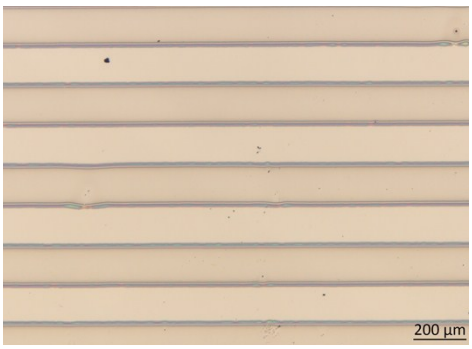

Figure S5. Zoom-in image of TFSA/POFPMA lines (3 layers) printed on flat graphene-covered Si substrates. The printed lines correspond to the slightly darker areas.

Table S2. The electrical parameters n, µ and R_s for two different samples of flat graphene-covered Si substrates (CVD grown graphene on copper and transferred to Si substrates) before and after doping with inkjet-printed TFSA/POFPMA lines (40 mM TFSA). The table presents data for 2 samples.

	Concentration Charge Carriers			Mobility			Sheet Resistance			
Concentration TFSA	n_{before}	n_{after}	Δn	μ_{before}	μ_{after}	$\Delta\mu$	$R_{S,before}$	$R_{S,after}$	ΔRs	Decrease Rs
(mM)	(cm^{-2})	(cm^{-2})	(cm^{-2})	($cm^2 V^{-1} s^{-1}$)	($cm^2 V^{-1} s^{-1}$)	($cm^2 V^{-1} s^{-1}$)	(Ω/sq)	(Ω/sq)	(Ω/sq)	(%)
40	2.21E+12	1.64E+13	1.42E+13	1393	709	-684	1508	512	-996	66
	2.68E+12	1.82E+13	1.55E+13	1068	470	-598	1779	730	-1049	59

References

[1] T. Ciuk, I. Pasternak, A. Krajewska, J. Sobieski, P. Caban, J. Szmidt, W. Strupinski, Properties of Chemical Vapor Deposition Graphe -684 ansferred by High-Speed Electrochemical Delamination, J. Phys. Chem. C. 117 (2013) 20833–20837.

doi:10.1021/jp4032139.

[2] Y. Wang, Y. Zheng, X. Xu, E. Dubuisson, Q. Bao, J. Lu, K.P. Loh, Electrochemical delamination of CVD-grown graphene film: Toward the recyclable use of copper catalyst, ACS Nano. 5 (2011) 9927–9933. doi:10.1021/nn203700w.

[3] J. Van Erps, T. Ciuk, I. Pasternak, A. Krajewska, W. Strupinski, S. Van Put, G. Van Steenberge, K. Baert, H. Terryn, H. Thienpont, N. Vermeulen, Laser ablation- and plasma etching-based patterning of graphene on silicon-on-insulator waveguides, Opt. Express. 23 (2015) 26639. doi:10.1364/OE.23.026639.

[4] A. Kütt, T. Rodima, J. Saame, E. Raamat, V. Mäemets, I. Kaljurand, I.A. Koppel, R.Y. Garlyauskayte, Y.L. Yagupolskii, L.M. Yagupolskii, E. Bernhardt, H. Willner, I. Leito, Equilibrium acidities of superacids, J. Org. Chem. 76 (2011) 391–395. doi:10.1021/jo101409p.